# Quantitative Evaluation of Misregistration Induced Color Shifts in Color Halftones

Basak Oztan[a], Gaurav Sharma[a] and Robert P. Loce[b]

[a]University of Rochester, Rochester, NY, USA
[b]Xerox Corporation, Webster, NY, USA

## ABSTRACT

Color-to-color misregistration refers to misregistration between color separations in a printed or display image. Such misregistration in printed halftoned images can result in several image defects, a primary one being shifts in average color. The present paper examines the variation in average color for two-color halftoned images as a function of color-to-color misregistration distance. Dot-on-dot/dot-off-dot and rotated dot screen configurations are examined via simulation and supported by print measurements. The color and color shifts were calculated using a spectral Neugebauer model for the underlying simulations. As expected, dot-on-dot/dot-off-dot color shifts were very high, while rotated dots screens exhibited very little color shift under the present idealized conditions. The simulations also demonstrate that optical dot gain significantly reduces the color shifts seen in practice.

**Keywords:** Misregistration, color printing, clustered dot halftoning, average color shift

## 1. INTRODUCTION

Color hardcopy reproduction commonly employs halftoning. Several halftoning technologies have been developed over the long and rich history of halftone reproduction. The earliest halftone image production method[1] is a photographic screening process that produces *clustered dots* having a pre-determined periodicity. Differing gray levels are reproduced in such a system through a change in the size of the individual dots. Clustered dot halftones are thus amplitude modulated (AM) signals in which the frequency of the dots is fixed but the size of the dots varies according to the gray level of the image. Digital halftoning using a computer offers a significantly increased set of options for halftoning. Not only can the traditional process be mimicked by using clustered-dot screens but it is also possible to produce dispersed dot screens and adaptively generated halftones either through sequential processing, such as *error-diffusion* or using iterative methods that optimize a suitably chosen cost function.[2–4] Despite the increased choices, clustered-dot halftoning continues to be the method of choice, for xerography and lithography, which are the two primary methods employed in high volume color printing. The primary reasons for the choice are the stability and predictability of clustered dots for these printing systems. For the current study on misregistration, we focus on xerographic printers, and therefore consider only clustered dot halftoning methods. Further, we restrict our attention to orthogonal halftone dots,[2] for which the cells are square in shape (either aligned with the natural coordinate system for the page or rotated).

In the printing of monochrome (single channel) images, the primary consideration is the visibility of the halftone textures, which is determined by the (fundamental) halftone frequency for clustered dot halftones that we consider. Even though the repetition frequency is a 2-D quantity, for orthogonal clustered dot screens, it is often specified as the number $f$ of halftone cells that can be fit within a linear inch. The 2-D repetition frequencies are then the orthogonal frequency vectors $\mathbf{f}_1 = (f, 0)$ and $\mathbf{f}_2 = (0, f)$ or a suitably rotated version there-of.

For color halftone printing, individual separations of the Cyan (C), Magenta (M), Yellow (Y), Black (K) colorants are halftoned and printed in overlay. Due to the interactions among colorants, one must account not only for the frequencies of the individual separation halftones but also for the sum and difference frequencies

Send correspondence to B. Oztan: E-mail: basak@ece.rochester.edu, Telephone: 1 585 275-8122, Address: Electrical and Computer Engineering Department, University of Rochester, Rochester, NY, 14627-0126, USA, WWW: www.ece.rochester.edu/projects/iplab

produced as a result of the overlay. This is referred as *color moiré*. The simplified linear frequency specification breaks down in this scenario and it is necessary to consider the 2-D frequency vectors for the individual separations and their vector sums and differences. It is desirable that all periodic components, with appreciable magnitude, produced from the halftones and their interactions be at sufficiently high frequencies in magnitude (or zero) in order to minimize visibility. While a number of frequency combinations can satisfy these requirements, additional considerations often impose further restrictions. One issue in particular is the impact of misregistration among the color separations that is encountered in the printing process, which results in a color shift from the original image.

One conventional solution to the misregistration induced color shift problem is to use rotated versions of a single orthogonal halftone screen for different separations. Ideally, the process of rotation randomizes the overlap among separations yielding a pattern which on average is invariant to misregistration. The problem of color moiré is concurrently solved by using orientations of 75°, 15° and 45° for C, M and K screens respectively. This orientation ensures that the sum and difference frequencies of 2/3 colorant combinations out of C, M and K are either zero or larger in magnitude than half the magnitude of the individual frequencies. This is desirable because these separations produce the most objectionable moiré.[5] Typically Y separation has 0° orientation and the least objectionable moiré interaction.

While the conventional solution for clustered dot halftoning addresses misregistration; it is sub-optimal in other respects. In particular, using other orientations may be advantageous in terms of color moiré and gamut considerations if the registration can be significantly improved.[2] For example, dot-on-dot halftones, which avoid moiré and are inexpensive since only one screen need to be stored, or a simple dot-off-dot method for two colorants can be developed. In dot-on-dot halftoning, colorants are printed using the same halftone screens, this maximizes the overlap among separations. On the contrary, in dot-off-dot halftoning the aim is to have minimal overlap between the separations.[6]

As electronic printers improve in registration several of these alternative halftoning methods may become feasible and offer advantages. However, in order to do this it is necessary to quantify the color error made due to misregistration. This paper is an attempt to quantify the color shifts induced by registration errors using a combination of modeling and simulation. For the work presented here we restrict our attention to two colorant dot-on-dot, dot-off-dot and rotated dot halftones. In Sec. 2, we first give examples of misregistration amounts for some common technologies and review earlier work in this area. We then explain our simulation method in detail in Sec. 3, and give simulation and experimental results by several tables and figures in Sec. 4. Finally, we draw conclusions in Sec. 5.

## 2. BACKGROUND

As stated in Sec. 1, individual separations are overlaid in color printing. In this process some misregistration is inevitable due to mechanical positioning errors.[4] In spite of the substantial improvement in the electronic printing technologies, most printers still can not achieve perfect registration. Table 1 shows examples of maximum expected misregistration amounts of some printing technologies. Note that for some technologies the maximum expected misregistration equals or exceeds half the halftone period, which means full range of all possible registrations can occur. However, current xerographic and ink jet technologies, especially when printing at relatively slow speeds, can achieve significantly smaller registration errors than those technologies.

For ideal colorants, whose absorption bands do not overlap, it can be shown that inter-separation misregistration errors do not cause any changes in the average color of the halftone.[8] Most colorants used in practice deviate from this ideal behavior and registration errors, therefore, lead to a change in average color for the halftone print. As indicated earlier, one motivation for the rotated dot screens is to randomize the overlap among colorants to make the average color invariant to registration errors. When the overlap among separations is truly random, the Demichel equations[9] apply. Amidror et al[10] have demonstrated that the Demichel equations, or equivalently, the assumption of randomized overlap in the overlay of multiple separations applies if and only if the frequency vectors of the individual separations are linearly independent (*non-singular*). The work extends earlier work by Rogers[11] which covered the more limited case of two separations. Both results are strictly applicable in the limiting case of an infinite *measuring aperture* and in practice frequency vectors that are close to linearly

| Method of Printing | Substrate | Halftone frequency ($cpi$) | Maximum Expected Misregistration ($\mu m$) |
|---|---|---|---|
| Sheet-fed offset | Gloss coated | 150 | 80 |
| Sheet-fed offset | Uncoated | 150 | 80 |
| Web-fed offset | Gloss coated | 150 | 100 |
| Web-fed offset | Uncoated commercial | 133 | 130 |
| Web-fed offset | Newsprint | 100 | 150 |
| Flexography | Coated | 133 | 150 |
| Flexography | Newsprint | 100 | 200 |
| Flexography | Kraft(corrugated, other) | 65 | 250 |
| Screen printing (wet-on-wet) | Fabric | any | 0 |
| Screen printing (dried) | paper, fabric, other | 100 | 150 |
| Gravure | Gloss coated | 150 | 80 |

**Table 1.** Expected maximum misregistration error for some printing technologies[7]

dependence would also result in violations of the Demichel assumptions and therefore variations in mean color over a finite measuring aperture.

In the conventional rotated halftone screen configuration for CMYK printing, the linear independence assumption holds for any combination of two separations, but it is violated in the overlay of the three C, M, and K separations. It is also readily seen that the linear independence assumption fails for dot-on-dot and two colorant dot-off-dot configurations. The overall impact of the failure of Demichel equations on average color is determined also by the colorant characteristics, as mentioned earlier, and, as we demonstrate later, on the light interaction with the paper substrate (*optical dot gain*). This aspect has received relatively limited attention in existing literature. The color shift between two registration configurations for the overlay of 3 rotated screens, corresponding respectively, to dot-centered and hole-centered rosettes, have been reported by Daels et al.[12]

It is known that two colorant dot-on-dot and dot-off-dot halftones demonstrate significant sensitivity to registration errors, whereas (as would be anticipated in view of results mentioned in the above paragraph) two colorant combinations in conventional rotated configurations are quite insensitive.[2] However, the range of variation and its dependence on the extent of misregistration have not been characterized. In this paper we use a combination of modeling and simulation to quantitatively characterize the shift in average color due to misregistration for two colorant dot-on-dot, dot-off-dot and rotated dot halftones as a function of a) the amount of misregistration, b) the area coverage of individual separations, and c) the optical dot gain, as modeled by the empirical Yule-Nielsen[13] modification.

## 3. SIMULATION MODEL FOR MISREGISTRATION ANALYSIS

An overview of the system to produce the color halftones from continuous tone (*contone*) CMYK image is shown in Fig. 1. We first model a single separation halftoning process, which produces a clustered dot single separation halftone image from a given single separation contone image. We generate 4 single separation halftone images for C, M, Y, K channels of the image. We then combine those individual separations and produce the CMYK halftone image using separation superposition.

Afterwards, we find the effect of misregistration on the average color of the image. We generate two halftone images, one is assumed to be perfectly registered and used as a reference. The other is generated with some misregistration with respect to the reference image. We apply a spectral Neugebauer model to find their spectrum and the difference between the average color of the images in CIELab space (in $\Delta E^*_{ab}$ units). In the following subsections, the process is explained in detail.

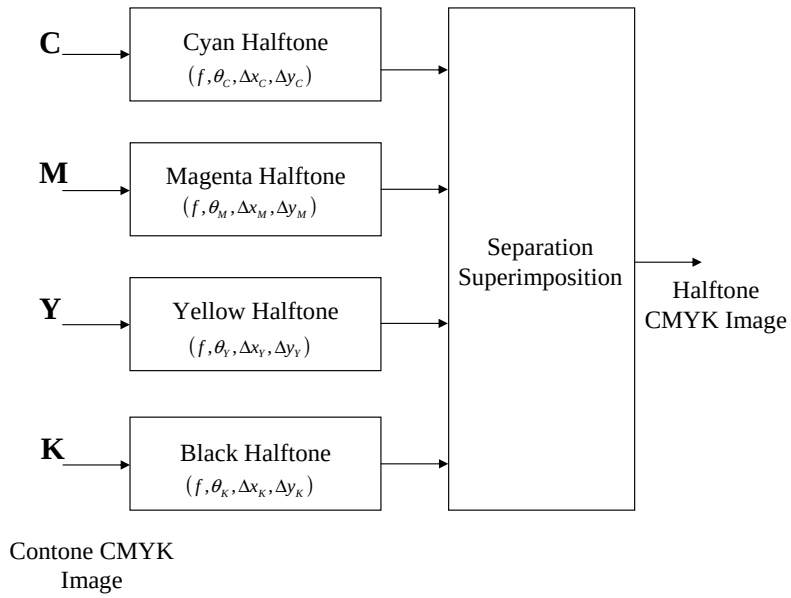


**Figure 1.** CMYK Halftone generation from a CMYK contone image

### 3.1. Individual Separation Halftone Generation

The process of halftoning a single separation is modeled as a point-wise comparison of the image value against a threshold function. In particular, we use an analytic halftone threshold function (often referred as *Euclidean spot function*) that is defined as[14, 15]:

$$K_T(x, y) = \frac{cos(2\pi f_x x) + cos(2\pi f_y y) + 2}{4}, \tag{1}$$

where $f_x$ and $f_y$ are the horizontal and vertical halftone frequencies and $x$ and $y$ are horizontal and vertical spatial positions, respectively. For orthogonal dots, the frequencies $f_x$ and $f_y$ are equal and given in terms of the linear frequency $f$ of the screen as $f_x = f$, $f_y = f$. The threshold function, thus, becomes

$$K_T(x, y) = \frac{cos(2\pi f x) + cos(2\pi f y) + 2}{4}, \tag{2}$$

To generate halftone images with different orientation and displacement, Eqn.2 can be modified as follows:

$$K_T(x, y; \theta, \Delta x, \Delta y) = \frac{cos(2\pi f(x' + \Delta x)) + cos(2\pi f(y' + \Delta y)) + 2}{4}\ , \tag{3}$$

where

$$\begin{bmatrix} x' \\ y' \end{bmatrix} = \begin{bmatrix} \cos(\theta) & \sin(\theta) \\ -\sin(\theta) & \cos(\theta) \end{bmatrix} \times \begin{bmatrix} x \\ y \end{bmatrix}, \tag{4}$$

$\theta$ is the rotation angle of the screen and $\Delta x$ and $\Delta y$ are the registration errors.

On the next step, the model superimposes this function with a normalized gray level value ($\delta \in [0, 1]$) to reproduce the gray level of the single separation contone image with the following rule:

$$H(\delta; K_T) = \begin{cases} 1 & \text{if } K_T(x_0, y_0) \leq \delta; \\ 0 & \text{if } K_T(x_0, y_0) > \delta, \end{cases} \tag{5}$$

where 1 and 0 correspond whether ink will be put on the position $(x_0, y_0)$ or not, respectively.

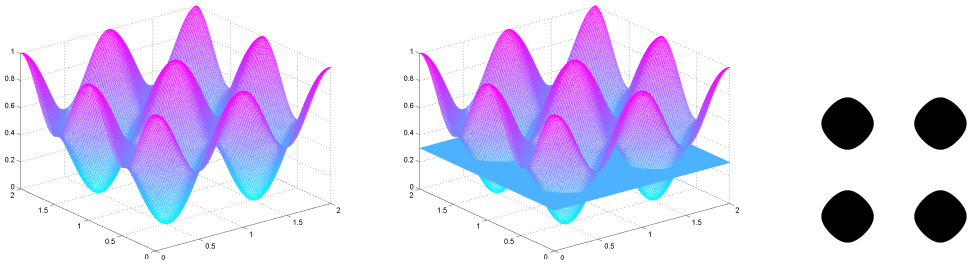

(a) (b) (c)

**Figure 2.** Single separation halftone generation. (a) shows the modified threshold function with $0^\circ$ of rotation, (b) shows the superposition of the function with the normalized gray value and (c) shows the generated single separation halftone dots

A mesh plot representing different stages of the process is shown in Fig. 2. Fig. 2.a shows the mesh plot of the threshold function $K_T$, Fig. 2.b shows the superposition of this function with the normalized gray level value $\delta$ and Fig. 2.c shows the generated halftone dots.

Both $\delta$ and $K \in [0, 1]$, however, due to the non-linearity of the cosine function, the relation between $\delta$ and $K$ is not a linear. Thus, comparison approximately generates the desired average gray level. Fig. 3 shows the relation between the generated fractional area and $\delta$. We denote the fractional area coverage $a$ as a function of the normalized gray level as $a = g(\delta)$.

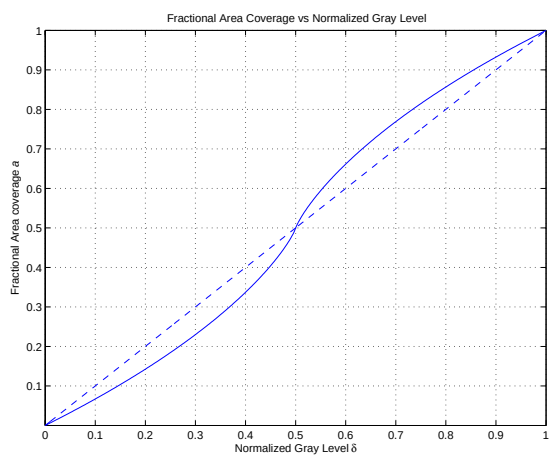


**Figure 3.** The relation between the fractional area coverage and normalized gray level. Note that $y = x$ line represents the ideal linear response

In our simulations, we compensate for the non-linearity of the response as shown in Fig. 4. To generate a single separation halftone with the fractional area coverage $a$, we first map that value to a normalized gray level $\delta$ using the inverse of the curve given in Fig. 3. The normalized gray level corresponding to a fractional area $a$ is thus computed as $\delta_a = g^{-1}(a)$. We generate the halftone image with the computed $\delta_a$.

### 3.2. Superposition of Multiple Separations

After the 4 single separation halftone images are obtained, they are fed to the corresponding printer channels and the separations are printed successively. This physically overlays the separations. In our simulations we simulate this process electronically using the color separation interaction model. The model takes the 4 single

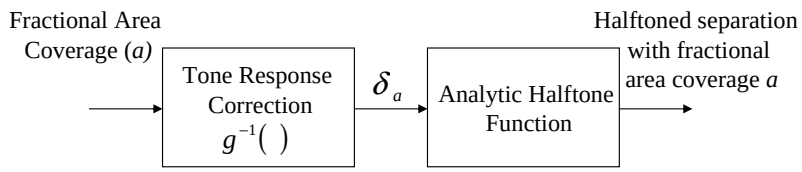


**Figure 4.** Generation of a halftone with fractional area coverage $a$

separation halftone images each corresponding to one of the CMYK channels and superimposes them. We use the common Neugebauer model assumptions for combining the separations. Since there are 4 colorants, there are $2^4 = 16$ possible colors that can be observed on the printed image.

In the actual printing, there is inevitable misregistration among the separations, which causes color shifts. It is obvious that if the same misregistration happens in all the separations, the average color does not change. Hence, the effect of misregistration can be studied by looking at the misregistration of other separations with respect to a chosen reference, which is assumed to be registered perfectly. Some examples of misregistration can be seen in Fig. 5.

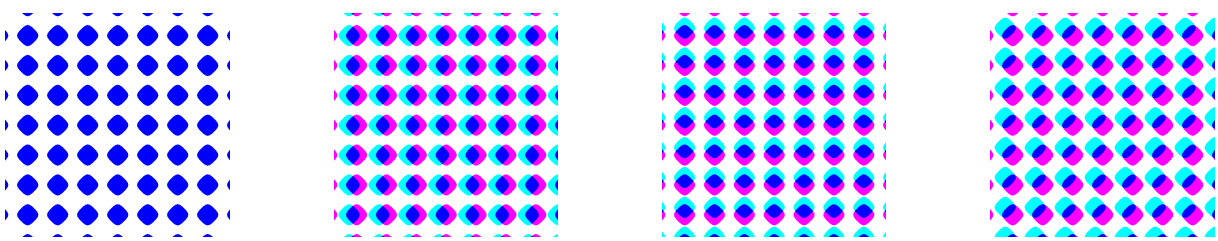

(a) (b) (c) (d)

**Figure 5.** Misregistration examples in dot-on-dot halftoning. (a) shows a perfect registered halftone, where (b), (c) and (d) shows misregistrations in horizontal, vertical and both directions respectively

In order to find the effect of misregistration on the average color, we generate two halftone images: one with all separations perfectly registered, i.e. $\Delta x = \Delta y = 0$ and the other with some misregistration. One of the separations of the misregistered halftone is generated with perfect registration in order to use it as a reference and the others with some registration error $\Delta x$ and $\Delta y$.

### 3.3. Calculation of the Average Color Shift

The process of calculating the the average color shift induced by misregistration can be seen in Fig. 6. After the original and the misregistered halftone images are generated, we use a spectral Neugebauer model[16] together with Yule-Nielsen correction[17] to predict their average spectrum. The spectral Neugebauer model is given by:

$$R_{avg}(\lambda) = \left( \sum_{i=1}^{16} a_i R_i^{\frac{1}{\gamma}}(\lambda) \right)^{\gamma}, \tag{6}$$

where $a_i$'s are the fractional areas, $R_i(\lambda)$'s are the spectrum of Neugebauer primaries and $\gamma$ is the empirical Yule-Nielsen correction factor.

The fractional areas, $a_i$'s, that are corresponding to the Neugebauer primaries are determined by pixel-counts instead of using Demichel equations in the simulations. As indicated earlier, the work of Amidror and Hersch indicates that the Demichel equations are inappropriate for the dot-on-dot and dot-off-dot configurations that we consider.[10]

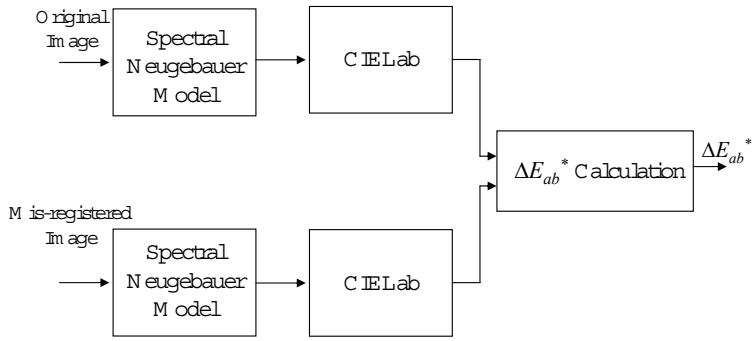


**Figure 6.** Average color shift computation from simulated misregistered images

In the next step, we find the Lab value of the average spectrum by first calculating the XYZ value from the average spectrum and then converting the corresponding XYZ value to Lab value.[18] Finally, we calculate the average color change in terms of $\Delta E^*_{ab}$ units with the following formula:

$$\Delta E^*_{ab} = \sqrt{(L_1 - L_2)^2 + (a_1 - a_2)^2 + (b_1 - b_2)^2)}, \tag{7}$$

where $L_1$, $a_1$, $b_1$ and $L_2$, $a_2$, $b_2$ are the CIELab values corresponding to the average spectrum in absence and presence of misregistration respectively.

### 3.4. Model calibration against Experimental Data

Since there is optical and physical dot gain effect in clustered dot halftone printing, dots appear to be larger on the hardcopy. Thus, we need to calibrate our model in order to make the simulations accurately. In the spectral Neugebauer model both $a_i$'s and $\gamma$ should be chosen adequately. For a fixed value of $\gamma$, we determine $a_i$'s using least squares. We generate single colorant ramp targets, which consist of several patches having fractional area coverages between [0, 1] and with approximately same fractional area coverage increments of a single separation, print them and measure their spectrum. For a single colorant halftone, the fractional area coverage is derived from the Neugebauer estimate of the spectrum as follows[19]:

$$\begin{aligned} R_a^{\frac{1}{\gamma}}\lambda &= aR_1^{\frac{1}{\gamma}}(\lambda) + (1-a)R_0^{\frac{1}{\gamma}}(\lambda) \\ R_a^{\frac{1}{\gamma}}\lambda - R_0^{\frac{1}{\gamma}}(\lambda) &= a\left(R_1^{\frac{1}{\gamma}}(\lambda) - R_0^{\frac{1}{\gamma}}(\lambda)\right) \end{aligned}$$

in vector form

$$\begin{aligned} (\overline{r}_a - \overline{r}_0) &= a\,(\overline{r}_1 - \overline{r}_0) \\ a &= \frac{\left((\overline{r}_a - \overline{r}_0)\,.\,(\overline{r}_a - \overline{r}_0)^T\right)}{||\,(\overline{r}_a - \overline{r}_0)\,||^2}, \end{aligned} \tag{8}$$

where $\overline{r}_a$ is the vector of samples of $R_a(\lambda)^{\frac{1}{\gamma}}$ and $a$ is the fractional area coverage. Other vectors are similarly defined.

The optimal value of $\gamma$ is then selected from a set of candidate values by determining the value that minimizes the mean square $\Delta E^*_{ab}$ color error over the entire set of multiple colorant ramps. This $\gamma$ is used throughout our simulations.

## 4. SIMULATION RESULTS

In this paper, we find the average color shift induced by misregistration for two colorant dot-on-dot, dot-off-dot and rotated dot halftoning. We carry out several simulations, as well as experiments, in which we print targets and measure their spectra using our model described in Sec. 3. Also, to verify the results we printed several test targets with perfectly registered and misregistered halftone patches, measured their spectra and found the maximum color shifts. Even though we assume they were printed with no registration error, misregistration occurs in the printing process. Thus, we only take the maximum average color shift cases to compare with the simulation results.

In the simulations, we choose the printer resolution as 4800 x 4800 dpi and the halftone frequency as 150 cpi. Hence, a full cell period is $\frac{4800}{150} = 32$ pixels on each side. The fractional pixel counts for the determination of the areas corresponding to the Neugebauer primaries clearly show some variation depending on the *simulated measurement aperture*, which corresponds to the size of images over which averaging is performed. We choose an effective measurement aperture of 0.5" x 0.5" square in our experiments, which corresponds to a 2400 x 2400 pixels image in our simulations.

The spectrum of 16 Neugebauer primaries is first measured and the value of the Yule-Nielsen parameter $\gamma$ is determined from individual colorant ramps as described in Sec. 3.4. Our experiments showed that $\gamma = 2.5$ gives the minimum error between the actual and Neugebauer estimate of the spectrum. In order to observe the effect of optical dot gain on the average color shift due to misregistration, 4 different $\gamma$ values are chosen and $\Delta E^*_{ab-max}$ as a function of fractional area coverage for dot-on-dot halftoning is found. The results are shown in Fig. 7. Note that, in the absence of optical dot gain ($\gamma = 1$), color shift is highly asymmetric. The dark regions appear significantly more sensitive to misregistration than the highlight regions. However, dot gain has the effect of reducing the error magnitude significantly, and also makes the error more symmetric with respect to fractional area coverage. Nevertheless, all the same, dark regions are slightly more sensitive than the highlight regions.

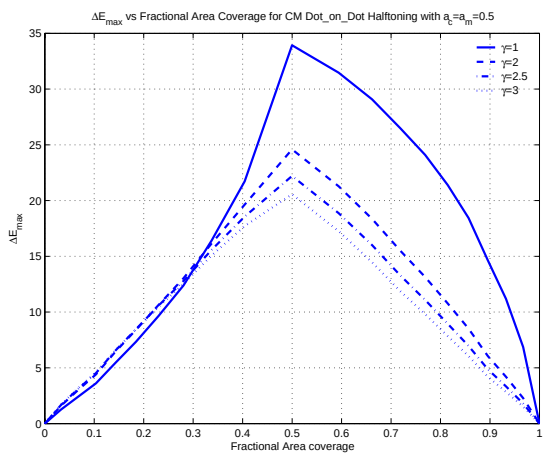


**Figure 7.** $\Delta E^*_{ab-max}$ vs. fractional area coverage for 4 different $\gamma$ values for CM dot-on-dot halftoning

In the simulations, first, we determined which fractional area coverage results in the highest average color shift if misregistration occurs. To simulate that, we assumed both colorants have same fractional area coverage and misregistration occurs in both horizontal and vertical directions with the same amount. We carry out several simulations, in which we vary both the fractional area coverages and misregistration amounts. Fig. 8.a shows the results that we have obtained for CM case. Fig. 8.b shows 4 different segments from Fig. 9.a to make the results more clear. The maximum average color shift occurs when $a_c = a_m = 0.5$ and $\Delta x = \Delta y = 85\mu m$, which is the half the period of the halftone for $f = 150$ cpi. It is obvious that when a shift equal to the half of the halftone period occurs in both directions, dot-on-dot halftoning transforms to dot-off-dot halftoning and vice versa. Table 2 shows the maximum values of $\Delta E^*_{ab}$ and the corresponding $\Delta L^*$, $\Delta a^*$ and $\Delta b^*$ values for all 2

colorant halftones in dot-on-dot and dot-off-dot halftones. It can be seen that the most sensitive combination to misregistration is YK in terms of maximum $\Delta E^*_{ab}$, however, in terms of $\Delta L^*$ and $\Delta a^*$ MK is the most sensitive combination.

| Colorants | $\Delta E^*_{ab\_max}$ for dot_on/off_dot halftoning | $\Delta L^*_{max}$ | $\Delta a^*_{max}$ | $\Delta b^*_{max}$ |
|---|---|---|---|---|
| CM | 22.08 | 12.33 | -13.69 | 12.17 |
| CY | 5.27 | 0.29 | 1.05 | -5.15 |
| CK | 29.91 | 16.77 | 14.44 | 20.12 |
| MY | 20.35 | 1.64 | -1.72 | -20.21 |
| MK | 36.99 | 19.48 | -30.91 | 5.76 |
| YK | 43.52 | 1.25 | 2.53 | -43.42 |

**Table 2.** Model's estimate for maximum values of $\Delta E^*_{ab}$ for dot-on-dot, dot-off-dot halftoning

Once we find the fractional area that yields the maximum color shift, we find the average color shift as a function of displacement. For this part of study, we fixed the fractional area coverages of the colorants to 0.5 and vary displacement amounts $\Delta x$ and $\Delta y$. Fig. 8.b shows the results for the CM dot-on-dot case. For all the other colorant combinations of dot-on-dot and dot-off-dot halftoning, this figure has the same profile with the amplitudes scaled with the maximum values of the average color shift given in Table 2. It can be seen that the maximum color shift occurs for $\Delta x = \Delta y =$ half period of the halftone. It can also be seen that the curve has symmetry around that point since a displacement higher than half period of the halftone can be treated as a negative displacement, which is equal to the difference between the displacement and half period of the halftone.

In the next step, to show the effect of misregistration in one direction we fix $\Delta y = 0$ and find the average color shift as a function of $\Delta x$ and fractional area coverages. Again, we assume both colorants have same fractional area coverage. Fig. 8.c shows the results for the CM dot-on-dot case. Fig. 9.b shows 4 different segments from Fig. 8.c to make the results more clear. For this case, the maximum value is less than the maximum value obtained from the previous cases. This result is expected since, in this case, the maximum point does not correspond to the transform from dot-on-dot to the dot-off-dot case.

For two colorant rotated screens, we expect almost no color shift with misregistration due to the validity of Demichel equations already mentioned earlier.[10] However, in order to have a parity check on our simulations, we follow the same procedure as for dot-on-dot and dot-off-dot screens. The relation between $\Delta E^*_{ab}$ and registration error in both horizontal and vertical direction for rotated CM dot screens is shown in Fig. 8.d. As expected, $\Delta E^*_{ab-max}$ is negligibly small compared to dot-on-dot and dot-off-dot screens.

To compare our simulation results against actual data, we electronically generated several test targets with a sampling of all possible misregistrations of up to half a period of the halftone. These were than printed and their spectra were measured with a spectrophotometer. Since the exact misregistration in the printer is unknown, this process ensures that we have a reasonable sampling of all misregistration in print (assuming the misregistration is similar over the page). From the individual measurements, average values and deviations with respect to the average computed for each patch in $\Delta E^*_{ab}$ units were computed. To compare this data with the simulation data, we used the fractional area coverages that we found using least squares approximation described in Sec. 3.4. Then, we used the algorithm described in Fig. 4 to find the normalized gray level values to generate the experimental halftone patches. Table 3 shows the results that we obtained from the experimental data and their corresponding model estimate. For most of the cases our estimates are close to the experimental data, however, for some cases due to print variations and measurement errors caused by aperture and noise in the system, model estimates do not give the actual data. In particular, the differences for the rotated screens are significantly higher than our estimates from simulations.

## 5. CONCLUSION

In this paper, we show the effect of misregistration on the average color for 2 colorant dot-on-dot, dot-off-dot and rotated dot halftones quantitatively. We show that darker regions are more sensitive to registration errors

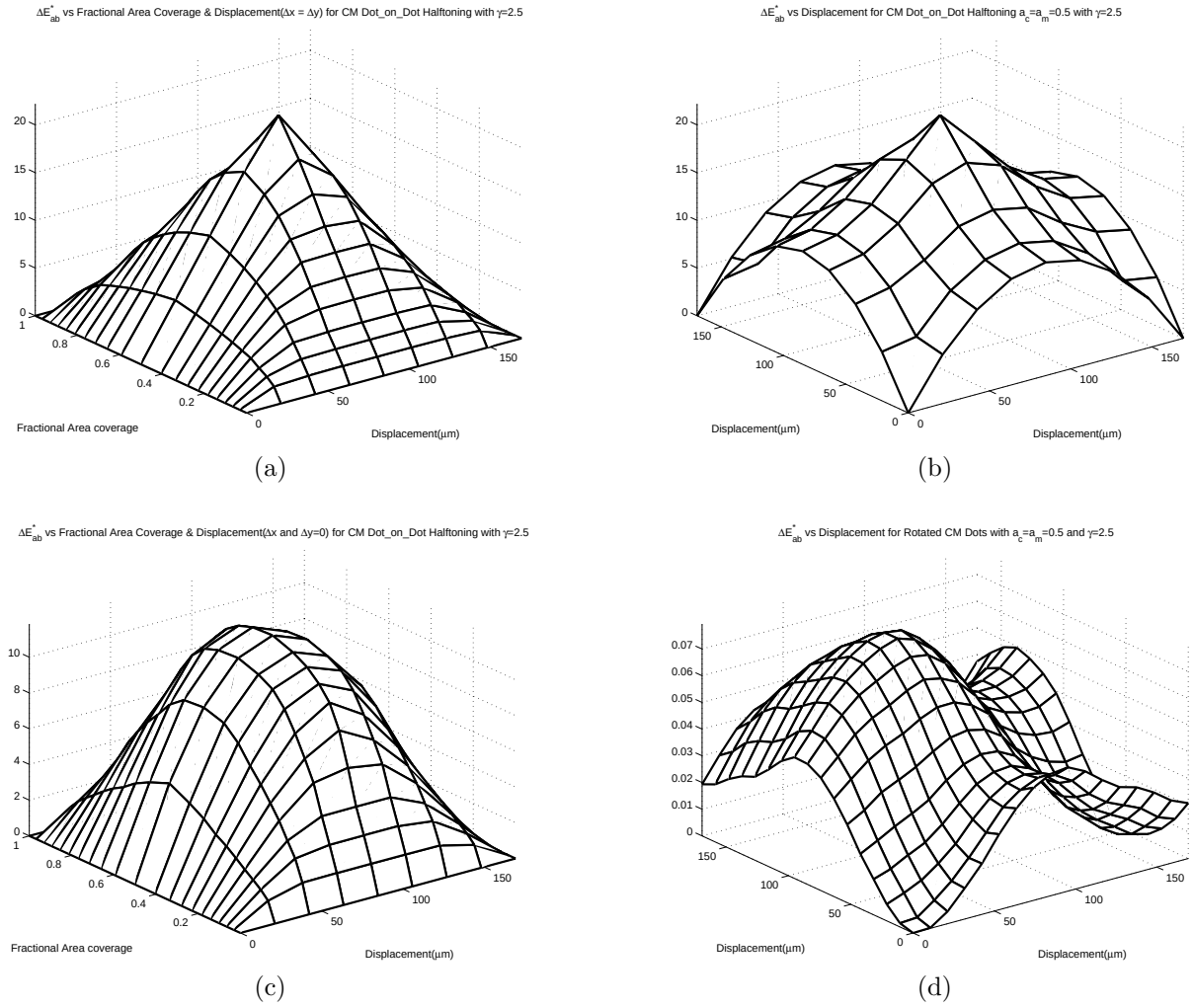


**Figure 8.** $\Delta E^*_{ab}$ vs (a) vs fractional area coverage and equal misregistration in both horizontal and vertical directions, (b) displacement in both horizontal and vertical directions for $a_c = a_m = 0.5$ fractional area coverage (c) fractional area coverage and misregistration in one direction only for CM dot-on-dot halftone and (d) displacement in both horizontal and vertical directions result for CM rotated dot halftone

than highlight regions. Also, we show that for 2 colorant dot-on-dot, dot-off-dot halftones YK combination is the most sensitive and CY combination is the least sensitive to misregistration. Furthermore, we show that Yule-Nielsen correction factor affects the results significantly. Our results show good agreement with experimental data gathered from actual prints.

In future work, we will characterize the effect of misregistration on the average color more comprehensively including 3 or more colorant halftones. The work can help the design of new methods for color halftoning, which are applicable in todays color printers with better registration performance and can also help in determining registration specifications.

## REFERENCES


1. W. H. F. Talbot, "Improvements in the art of engraving." British Patent Specification No. 565, 29 Oct. 1852.
2. C. M. Hains, S. Wang, and K. T. Knox, "Digital color halftones," in Sharma.[20] Chapter 6.

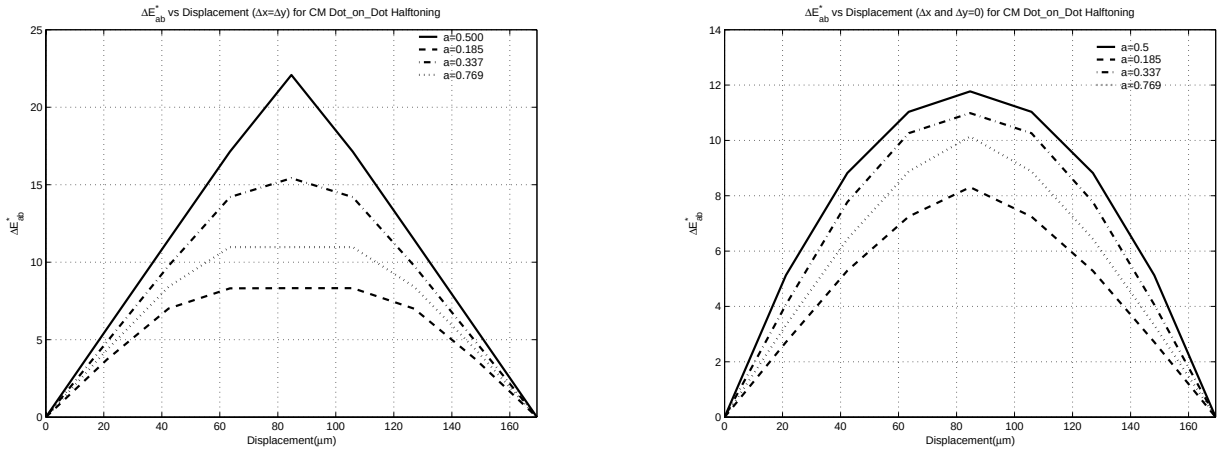


(a) (b)

**Figure 9.** 4 different segments of (a) Fig. 8.a, (b) Fig. 8.c to make them clear

| Colorant | Halftone Technique | Measured $\Delta E^*_{ab\_max}$ | Model Estimate $\Delta E^*_{ab\_max}$ |
|---|---|---|---|
| CM | Dot-on-dot | 12.6564 | 12.3059 |
| | Dot-off-dot | 9.9458 | 12.3059 |
| | Rotated | 3.6071 | 0.0605 |
| CY | Dot-on-dot | 13.0659 | 2.8153 |
| | Dot-off-dot | 13.1397 | 2.8153 |
| | Rotated | 5.6231 | 0.099 |
| CK | Dot-on-dot | 17.8162 | 17.2092 |
| | Dot-off-dot | 15.4894 | 17.2092 |
| | Rotated | 4.1735 | 0.0040 |
| MY | Dot-on-dot | 15.3783 | 12.3502 |
| | Dot-off-dot | 15.1940 | 12.3502 |
| | Rotated | 7.3462 | 0.0216 |
| MK | Dot-on-dot | 18.3357 | 25.5797 |
| | Dot-off-dot | 17.0103 | 25.5797 |
| | Rotated | 5.3181 | 0.0023 |
| YK | Dot-on-dot | 27.6846 | 26.4116 |
| | Dot-off-dot | 24.7431 | 26.4116 |
| | Rotated | 6.1881 | 0.0100 |

**Table 3.** Comparison of the experimental results and the model estimate


3. T. Pappas, J. P. Allebach, and D. Neuhoff, "Model-based digital halftoning," pp. 14–27.
4. A. U. Agar, F. A. Baqai, and J. P. Allebach, "Human visual model based color halftoning," in Sharma.[20] Chapter 7.
5. I. Amidror, R. D. Hersch, and V. Ostromoukhov, "Spectral analysis and minimization of moiré patterns in color separation," *J. Electronic Imaging* **3**, pp. 295–317, Jul. 1994.
6. H. R. Kang, *Digital Color Halftoning*, IEEE Press, Piscataway, NJ, 1999.
7. B. Lawler, *The Complete Guide to Trapping*, Hayden Books, second ed., 1995.
8. J. A. C. Yule, *Principles of color reproduction, applied to photomechanical reproduction, color photography, and the ink, paper, and other related Industries*, Wiley, New York, 1967.
9. E. Demichel in *Procédé*, **26**, pp. 17–21,26–27, 1924.

10. I. Amidror and R. D. Hersch, "Neugebauer and demichel: Dependence and independence in n-screen superpositions for colour printing," *Color Res. Appl.* **25**, pp. 267–277, Aug. 2000.
11. G. L. Rogers, "Neugebauer revisited: Random dots in halftone screening," *Color Res. Appl.* **23**, pp. 104–113, Jan. 1998.
12. K. Daels and P. Delabastita, "Color balance in conventional halftoning," in *TAGA Proc.*, pp. 1–18, 1994.
13. J. A. C. Yule and W. J. Neilsen[sic], "The penetration of light into paper and its effect on halftone reproduction," in *TAGA Proc.*, pp. 65–76, 7-9 May 1951.
14. R. J. Pellar and L. Green, "Electronic halftone generator." United States Patent No. 4 149 183, 1979.
15. R. J. Pellar, "Electronic halftone generator." United States Patent No. 4 196 451, 1980.
16. K. Sayangi, ed., *Proc. SPIE: Neugebauer Memorial Seminar on Color Reproduction*, vol. 1184, SPIE, Bellingham, WA, 14-15 Dec. 1989.
17. R. Balasubramanian, "Optimization of the spectral neugebauer model for printer characterization," *J. Electronic Imaging* **8**, pp. 156–166, Apr. 1999.
18. G. Sharma, "Color fundamentals for digital imaging," in *Digital Color Imaging Handbook*.[20] Chapter 1.
19. M. Xia, E. Saber, G. Sharma, and A. M. Tekalp, "Total least squares regression in neugebauer model parameter estimation for dot-on-dot halftone screens," in *Proc. IS&T NIP14: Intl. Conf. Dig. Printing Technologies*, pp. 281–284, 18-23 Oct. 1998.
20. G. Sharma, ed., *Digital Color Imaging Handbook*, CRC Press, Boca Raton, FL, 2003.